Journal of Science and Technology in Civil Engineering, HUCE (NUCE), 2022, 16 (3): 46–58

EFFECT OF SPATIAL VARIABILITY OF CREEP ROCK ON THE STABILITY OF A DEEP DOUBLE-LINED DRIFT

Tran Ngoc Tuyen[a,b,*], Duc-Phi Do[b], Dashnor Hoxha[b], Minh-Ngoc Vu[c], Gilles Armand[c]

[a] *Faculty of Engineering - Technology, Ha Tinh University, Cam Xuyen district, Ha Tinh province, Vietnam*
[b] *Univ Orléans, Univ Tours, INSA CVL, Lamé, EA 7494, France*
[c] *Andra, R&D Division, 92298 Chatenay-Malabry, France*

Article history:
Received 11/01/2022, Revised 24/6/2022, Accepted 24/6/2022

Abstract

This work aims at investigating the effect of aleatoric uncertainty of creep rock properties on the stability of an underground structure. This uncertainty relates to the spatial variability of the mechanical parameters representing the time-dependent behavior of geological rock formation due to the change in its mineralogy. The chosen methodology consists of representing the aleatoric uncertainty of rock properties by random fields, written as correlation functions with respect to the spatial correlation length. The adaptation of the well-known Expansion Optimal Linear Estimation method (EOLE) is performed to account for the cross-correlation of the random fields of the viscoplastic parameters of the host rock. Then, the Kriging-based reliability analysis is undertaken with respect to the discretized random fields, which allows elucidating the effect of spatial variability. As an application, the proposed approach is chosen to study the stability in the long-term of a deep double-lined drift within the geological disposal facilities (Cigeo project) conducted by the French National Radioactive Waste Management Agency (Andra). The drift will be excavated in Callovo-Oxfordian (COx) claystone (if the Cigeo project is licensed), considered as a potential host rock for the deep geological nuclear waste disposal in France. The results show that the chosen Kriging metamodel for the reliability analysis can be appropriate for the case of high correlation length represented by a moderate number of random variables (up to about 50) after the discretization of random fields. Further, the consideration of aleatoric uncertainty exhibits a lower probability of exceedance in comparison with the case where spatial variability is ignored. Still, more investigations need to be conducted in the future to conclude this observation.

Keywords: spatial variability; aleatoric uncertainty; random field; EOLE; deep drift; viscoplastic behavior; Kriging-based reliability analysis.

https://doi.org/10.31814/stce.huce(nuce)2022-16(3)-04

1. Introduction

In geotechnical engineering applications, the mechanical properties of geological formation are uncertain, and they naturally vary in space. Such aleatory uncertainty related to inherent spatial variability can strongly affect the geotechnical structure's response [1–4] and hence their stability during and after construction as well as in the long term [5, 6]. Using the reliability analysis, the authors in [7] show, for instance, that ignoring the spatial variability of rock properties often underestimates the probability of failure (P_f) of a slope. It could be more dangerous in case of significant uncertainty characterized by the high coefficients of variation (COVs) of the random parameters.

*Corresponding author. *E-mail address:* tuyen.tranngoc@htu.edu.vn (Tuyen, T. N.)

In recent years, the variability of mechanical properties in space has received much attention. For example, Yu et al. [8] took advantage of stochastic numerical modeling to study the performance of tunnel linings and concluded that this procedure could lead to a more equitable and economical design. Besides, the well-known Monte Carlo Simulation (MCS) can be combined with numerical analysis to introduce spatially variable soil properties described by random fields [9, 10]. Similar research works were also conducted in rock formation [11–13]. In their study, Song et al. [13] investigated the effect of spatial variability in rock mass properties on soil deformation due to tunneling. However, to the best of the authors' knowledge, no work has yet been dedicated to studying the effect of spatial variability of rock time-dependent on the behavior of the liner.

For describing the spatial variability of a random variable, the random field concept has been largely used [10–13]. Mathematically, a random field can be expressed in the form of a correlation function (such as a Markovian or Gaussian function) with an essential characteristic parameter, the spatial correlation length. For the numerical modeling (i.e., direct evaluation of the performance function), this random field needs to be discretized by an appropriate technique. After the discretization of all random fields, the probabilistic assessment can be undertaken as an uncertainty problem tackled in typical structural reliability analysis problems (see [14–16] and different references cited therein). However, most contributions in the literature focused on the aleatoric uncertainty of the short-term behavior of rock formation using the elastoplastic model. Several attempts were conducted to account for the uncertainty effect on tunnel stability in the long term of about 100 years [17–19], but these studies neglected the variability in the space of the creep rocks. Therefore, the primary purpose of this paper is to investigate the effect of the spatial variability of the time-dependent behavior of the rock mass on the stability at long-term of a deep tunnel. More precisely, the application is conducted on the deep drift excavated in the Callovo-Oxfordian (COx) claystone, a potential host formation for geological radioactive waste disposal in France.

This work is organized as follows. Firstly, a brief description of the problem related to drift support stability is illustrated. Next, we present an appropriate technique to discretize the cross-correlated random fields representing the spatial variability of viscoplastic parameters of COx claystone. Then a metamodeling technique based on the Kriging surrogate, the modified AK-MCS recently presented in [6, 17–20], is chosen for the reliability analysis of deep drift. Comparing these obtained results with the ones of the classical uncertainty problem (i.e., ignoring the aleatoric uncertainty) exhibits the effect of spatial variability and the limit of the chosen Kriging metamodel to tackle the problem of high dimension.

2. Problem statement and procedure to handle the spatial variability

2.1. Description of the considered problem

As a reminder, this study considers the effect of spatial variability of time-dependent host rock properties on the long-term stability of a tunnel in the context of a geological disposal facility during the operational phase (∼100 years). The geometry model and boundary condition, and loading is shown in Fig. 1. Detail about the considered problem can be found in our previous works (see [18] for more details). Herein, we only summarize the main characters of this problem. The tunnel is excavated at a depth of about 500 m, corresponding to far-field stress σ_0 = 12.5 MPa, within the Callovo-Oxfordian claystone. This host rock exhibits time-dependent behavior, which is usually modeled by Lemaitre law to reproduce the data tests from both in-situ experiments and laboratory tests on samples [21, 22]. Lemaitre model is characterized by three parameters A, B, and C. The drift is supported by a concrete lining C60/75 (thickness l_2), separated from the rock mass by a compressible layer (thickness l_1). The compressible material layer allows absorbing the convergence of the host rock, which increases as a function of time due to the creep behavior of the COx claystone. This innovative design helps reduce the radial stress transmitted to the concrete lining, reducing the project's cost. The concrete liner is assumed to be elastic, while the compressible material is tri-linear elastic (see [18] for the detail of constitutive models for these three materials).

Compared with the problem tackled in our previous works [17–19], the spatial variability of host rock properties (i.e., the surrounding rock mass of the underground structure is heterogeneous) is accounted for in this study. Although the spatial variability problem needs to be modeled in three-dimensional (3D), we adopt the 2D plane-strain model to simplify the numerical simulation in terms of computational time. The excavation is modelled by the well-known convergence-deconfining method.

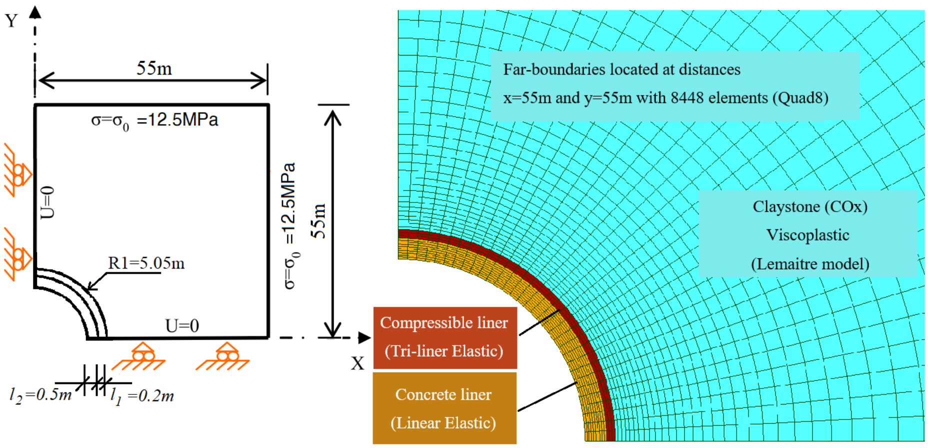

Figure 1. 2D-plan strain model of drift supported by double linings in viscoplastic COx claystone

As the study in [18], the deep drift support's exceedance probability at the period of exploitation of 100 years will be evaluated by the reality analysis using metamodeling techniques such as the modified AK-MCS method. However, we consider in this paper the aleatoric uncertainty of the viscoplastic behavior of the host rock characterized by the Lemaître model, whose description can be found in [18]. Following that, the spatial variability of four random parameters (three coefficients A, B, and C of the Lemaître model and Young modulus E) are represented by four random fields, each of which can be characterized by a proper correlation length. Nevertheless, for the methodology verification purpose, and since all the data concerning the correlation length of the mechanical properties of COx rock are not available, we assume that all four random fields have the same correlation length. With respect to the studies in [17–19], the challenges of the considered aleatoric uncertainty problem relate not only to the time-dependent behavior of the host rock but also to the consideration of the cross-correlation relationships between the three parameters of the Lemaître model as observed in [18].

2.2. *Discretization of random fields by the EOLE method*

In the geotechnical engineering field, the increasing interest in probability analysis concerning spatial variability (or space-variant properties) points out the problem of achieving a reliable discretization of random fields. An appropriate discretization procedure permits replacing a continuous random field with a reasonable finite set of random variables that the underground structures' response can be assessed by the direct numerical evaluation (i.e., solving the deterministic problem using the finite element open-source *Code-Aster*). The precision of discretization is a crucial point for any subsequent probabilistic investigation.

In practice, it is not straightforward to sample a Gaussian random field $H(\mathbf{x}, \omega)$ to obtain the realization of H. Consequently, the discretization procedure is appeared to approximate the random field $H(\mathbf{x}, \omega)$ by $\hat{H}(\mathbf{x}, \varpi)$. The methods of discretization can be divided into three groups [23–25], namely: point discretization [26], average discretization [7, 27], and series expansion methods [28–31]. In which the series expansion methods commonly used in the literature can be listed as Karhunen-Loève expansion (KLE), orthogonal series expansion (OSE), and the expansion optimal linear estimation method (EOLE) [20, 21]. The crucial point here is that the random target functions can be adequately simulated by serial expansion methods using a finite number of deterministic processes and random variables-coefficients. These methods are highly appreciated for complex problems. Corresponding to our studied problem, the latter method (i.e., the EOLE) is suitable thanks to its accuracy, more practical, and efficiency than some other series expansion discretization techniques according to [32].

The EOLE method can be used to approximate the Gaussian stochastic input parameters [20, 21]. On the basis of the pointwise regression of the original random field with respect to the selected values of the field and compaction of the data by spectral analysis [23, 33], the subsequent problem takes into account the derivation of an EOLE of a random field with two aims: (a) limit the computational effort devoted to the application of the resulting representation; and (b) ensure the representation meets all accuracy standards. The first objective can be achieved by limiting the highest order of the expansion term and the total number of random variables used to construct a representation. In contrast, the second goal will be attained by finding the minimum of multiple error estimators.

The EOLE method also has the advantage of allowing the error variance of the corresponding discretization scheme to be determined. Thus, one can determine the optimal number of eigenmodes for a specified value of error variance. Notice that this discretization method conducts an expression that gives the random field's value at each point in the space of the rock mass as a function of N random variables (following the standard normal distribution law) which equals the number of eigenmodes. For a given value of the error variance on the EOLE, the number N is small for high values of autocorrelation distances [30]. The homogeneous medium is a particular case according to the autocorrelation distances get infinite value. However, N can be extremely valuable when the autocorrelation distances are so small [34].

Mathematically, the EOLE method represents a stochastic field in terms of a linear combination of deterministic functions/vectors $H(\mathbf{x}, \theta)$ and a finite set of uncorrelated standard Gaussian random variables $\phi_j(\theta)$ where θ stands for the random nature. Let us denote by $\boldsymbol{\chi}$ the random vector $\{H(\mathbf{x}1), ..., H(\mathbf{x}N)\}$. By construction, $\boldsymbol{\chi}$ is a Gaussian vector whose mean value $\boldsymbol{\mu}_\chi$ and covariance matrix $\boldsymbol{\Sigma}_{\chi\chi}$ is expressed as:

$$\boldsymbol{\mu}_\chi^j = \mu(\mathbf{x}_j) \tag{1}$$

$$\left(\boldsymbol{\Sigma}_{\chi\chi}\right)_{j,k} = Cov\left[H(\mathbf{x}_j), H(\mathbf{x}_k)\right] = \sigma(\mathbf{x}_j)\sigma(\mathbf{x}_k)\rho(\mathbf{x}_j, \mathbf{x}_k) \tag{2}$$

The EOLE of random variable $H(\mathbf{x})$ onto the random vector $\boldsymbol{\chi}$ reads:

$$H(\mathbf{x}) \approx \hat{H}(\mathbf{x}) = \mu(\mathbf{x}) + \boldsymbol{\Sigma}_{H\chi}^T(\mathbf{x}) \cdot \boldsymbol{\Sigma}_{\chi\chi}^{-1} \cdot (\boldsymbol{\chi} - \boldsymbol{\mu}_\chi) \tag{3}$$

where: $\boldsymbol{\Sigma}_{H(\mathbf{x})\chi}(\mathbf{x})$ is a vector whose components are given by

$$\boldsymbol{\Sigma}_{H(\mathbf{x})\chi}^j(\mathbf{x}) = Cov\left[H(\mathbf{x}), \chi_j\right] = Cov\left[H(\mathbf{x}), H(\mathbf{x}_j)\right] \tag{4}$$

Based on the non-accumulation of eigenvalues λ_j, around a non-zero value, one can order them in a descending series converging to zero. Let us consider the spectral decomposition of the covariance matrix $\mathbf{\Sigma}_{\chi\chi}$:

$$\mathbf{\Sigma}_{\chi\chi}\boldsymbol{\phi_j} = \lambda_j \phi_j \quad j = 1, ..., N \tag{5}$$

This equation allows one to transform the original vector linearly $\boldsymbol{\chi}$:

$$\boldsymbol{\chi}(\theta) = \boldsymbol{\mu}_\chi + \sum_{j=1}^{N} \sqrt{\lambda_j}\xi_j(\theta)\phi_j \tag{6}$$

where $\left\{\xi_j, j = 1, ..., N\right\}$ are independent standard normal variables. Substituting for Eq. (4.6) in (3) and solving the OLE problem in Eq. (5) yields the EOLE representation of the random field:

$$H(\mathbf{x}, \theta) \approx \hat{H}(\mathbf{x}, \theta) = \mu(\mathbf{x}) + \sum_{j=1}^{N} \frac{\xi_j(\theta)}{\sqrt{\lambda_j}}\phi_j^T \mathbf{\Sigma}_{H(\mathbf{x})\boldsymbol{\chi}} \tag{7}$$

By defining the variance of $H(\mathbf{x})$ is $\sigma^2(\mathbf{x})$, the error variance for EOLE after basic algebra is:

$$Var[H(\mathbf{x}) - \hat{H}(\mathbf{x})] = \sigma^2(\mathbf{x}) - \sum_{j=1}^{N} \frac{1}{\lambda_j}\left(\phi_j^T \mathbf{\Sigma}_{H(\mathbf{x})\boldsymbol{\chi}}\right)^2 \tag{8}$$

In Eq. (8), the second term is identical to the variance of $\hat{H}(\mathbf{x})$. Thus, EOLE always underestimates the exact variance. However, the error decreases monotonically with N, which helps one automatically define the cut-off value of N for a provided tolerance in the variance error.

2.3. Discretization of the cross-correlated random fields

In engineering practice, the parameters of random fields and their cross-correlation, which are often unknown, must be estimated from extensive measurements. Thus, it is a high challenge to either precisely approximate random field parameters or correctly simulates cross-correlated random field samples (RFSs) since the number of measurements is sparse and limited (due to sensor failure, budget limit, etc.) [35].

In this study, the cross-correlated random fields that characterize the spatial variability of the viscoplastic parameters of COx claystone are discretized by the EOLE method. Due to the independence of the Young modulus (E), its random field can be discretized directly using Eq. (7). The three coefficients (i.e., A, B, and C of the Lemaître model) have a cross-correlation between each pair. Thus, cross-correlation coefficients define the cross-correlation structure between each pair of simulated fields. The method requires all cross-correlated fields on the domain to share an identical autocorrelation function, the adopted assumption in this work (see also [15]).

Considering now three cross-correlated random fields of the coefficients A, B, and C of the Lemaître model, the cross-correlation matrix reads:

$$\left[\hat{\mathbf{C}}\right] = \begin{bmatrix} 1 & \rho_{AB} & \rho_{AC} \\ \rho_{AB} & 1 & \rho_{BC} \\ \rho_{AC} & \rho_{BC} & 1 \end{bmatrix} = \begin{bmatrix} \Phi_{11}^{\mathbf{C}} & \Phi_{12}^{\mathbf{C}} & \Phi_{13}^{\mathbf{C}} \\ \Phi_{21}^{\mathbf{C}} & \Phi_{22}^{\mathbf{C}} & \Phi_{23}^{\mathbf{C}} \\ \Phi_{31}^{\mathbf{C}} & \Phi_{32}^{\mathbf{C}} & \Phi_{33}^{\mathbf{C}} \end{bmatrix} \begin{bmatrix} \lambda_1^{\mathbf{C}} & 0 & 0 \\ 0 & \lambda_2^{\mathbf{C}} & 0 \\ 0 & 0 & \lambda_3^{\mathbf{C}} \end{bmatrix} \begin{bmatrix} \Phi_{11}^{\mathbf{C}} & \Phi_{12}^{\mathbf{C}} & \Phi_{13}^{\mathbf{C}} \\ \Phi_{21}^{\mathbf{C}} & \Phi_{22}^{\mathbf{C}} & \Phi_{23}^{\mathbf{C}} \\ \Phi_{31}^{\mathbf{C}} & \Phi_{32}^{\mathbf{C}} & \Phi_{33}^{\mathbf{C}} \end{bmatrix}^T \tag{9}$$

i.e.,

$$\left[\hat{\mathbf{C}}\right] = \left[\mathbf{\Phi}^{\mathbf{C}}\right]\left[\mathbf{\Lambda}^{\mathbf{C}}\right]\left[\mathbf{\Phi}^{\mathbf{C}}\right]^{T} \tag{10}$$

where $\left[\mathbf{\Phi}^{\mathbf{C}}\right]$: matrix of the eigenvector of the cross-correlation matrix $\left[\hat{\mathbf{C}}\right]$ of three variables A, B, C; $\left[\mathbf{\Lambda}^{\mathbf{C}}\right]$: matrix of the eigenvalue (diagonal matrix) of the cross-correlation matrix $\left[\hat{\mathbf{C}}\right]$; Superscripts T denotes the transpose of the matrix or vector.

It is denoted $\mathbf{I}_N$ as a unity matrix of the order N (after ordering the vectors by decreasing eigenvalues). We can define the orthonormal eigenvectors of the correlation matrix ($\mathbf{\Phi}^D$) as below:

$$\mathbf{\Phi}^D = \begin{bmatrix} \Phi_{11}^{\mathbf{C}}\mathbf{I}_N & \Phi_{12}^{\mathbf{C}}\mathbf{I}_N & \Phi_{13}^{\mathbf{C}}\mathbf{I}_N \\ \Phi_{21}^{\mathbf{C}}\mathbf{I}_N & \Phi_{22}^{\mathbf{C}}\mathbf{I}_N & \Phi_{23}^{\mathbf{C}}\mathbf{I}_N \\ \Phi_{31}^{\mathbf{C}}\mathbf{I}_N & \Phi_{32}^{\mathbf{C}}\mathbf{I}_N & \Phi_{33}^{\mathbf{C}}\mathbf{I}_N \end{bmatrix} \tag{11}$$

and,

$$\mathbf{\Lambda}^D = diag\left(\lambda_1^{\mathbf{C}}\mathbf{I}_N \quad \lambda_2^{\mathbf{C}}\mathbf{I}_N \quad \lambda_3^{\mathbf{C}}\mathbf{I}_N\right) \tag{12}$$

Then, the cross-correlation block sample matrix is defined as

$$\boldsymbol{\chi}_j^D(\theta) = \left[\boldsymbol{\phi}^D\right]_{3N\times 3N}\left[\left(\mathbf{\Lambda}^D\right)^{1/2}\right]_{3N\times 3N}\{\boldsymbol{\xi}\}_{3N\times 1} \tag{13}$$

i.e.,

$$\begin{aligned}\boldsymbol{\chi}_j^D(\theta) = \begin{bmatrix} \chi_{A,j}^D(\theta) \\ \chi_{B,j}^D(\theta) \\ \chi_{C,j}^D(\theta) \end{bmatrix} &= \begin{bmatrix} \Phi_{11}^{\mathbf{C}} & \Phi_{12}^{\mathbf{C}} & \Phi_{13}^{\mathbf{C}} \\ \Phi_{21}^{\mathbf{C}} & \Phi_{22}^{\mathbf{C}} & \Phi_{23}^{\mathbf{C}} \\ \Phi_{31}^{\mathbf{C}} & \Phi_{32}^{\mathbf{C}} & \Phi_{33}^{\mathbf{C}} \end{bmatrix}\begin{bmatrix} \sqrt{\lambda_1^{\mathbf{C}}}I_N & 0 & 0 \\ 0 & \sqrt{\lambda_2^{\mathbf{C}}}I_N & 0 \\ 0 & 0 & \sqrt{\lambda_3^{\mathbf{C}}}I_N \end{bmatrix}\begin{Bmatrix} \left\{\xi^{\mathbf{A}}\right\}_{N\times 1} \\ \left\{\xi^{\mathbf{B}}\right\}_{N\times 1} \\ \left\{\xi^{\mathbf{C}}\right\}_{N\times 1} \end{Bmatrix} \\ &= \begin{bmatrix} \Phi_{11}^{\mathbf{C}}\sqrt{\lambda_1^{\mathbf{C}}}I_N & \Phi_{12}^{\mathbf{C}}\sqrt{\lambda_2^{\mathbf{C}}}I_N & \Phi_{13}^{\mathbf{C}}\sqrt{\lambda_3^{\mathbf{C}}}I_N \\ \Phi_{21}^{\mathbf{C}}\sqrt{\lambda_1^{\mathbf{C}}}I_N & \Phi_{22}^{\mathbf{C}}\sqrt{\lambda_2^{\mathbf{C}}}I_N & \Phi_{23}^{\mathbf{C}}\sqrt{\lambda_3^{\mathbf{C}}}I_N \\ \Phi_{31}^{\mathbf{C}}\sqrt{\lambda_1^{\mathbf{C}}}I_N & \Phi_{32}^{\mathbf{C}}\sqrt{\lambda_2^{\mathbf{C}}}I_N & \Phi_{33}^{\mathbf{C}}\sqrt{\lambda_3^{\mathbf{C}}}I_N \end{bmatrix}\begin{Bmatrix} \left\{\xi^{\mathbf{A}}\right\}_{N\times 1} \\ \left\{\xi^{\mathbf{B}}\right\}_{N\times 1} \\ \left\{\xi^{\mathbf{C}}\right\}_{N\times 1} \end{Bmatrix}\end{aligned} \tag{14}$$

Here, each field is created using a set of independent random variables. These sets are then correlated with the assumed cross-correlation matrix between three expanded random fields according to the framework presented by Vořechovský [36]. Thus, the EOLE representation Gaussian random field in Eq. (7) can be rewritten as follows:

$$\begin{cases} H_A(\mathbf{x},\theta) \approx \hat{H}_A(\mathbf{x},\theta) = \mu_A + \sigma_A \displaystyle\sum_{j=1}^{N} \frac{\chi_{A,j}^D(\theta)}{\sqrt{\lambda_j}}\phi_j^T \Sigma_{H(\mathbf{x})\chi} \\ H_B(\mathbf{x},\theta) \approx \hat{H}_B(\mathbf{x},\theta) = \mu_B + \sigma_B \displaystyle\sum_{j=1}^{N} \frac{\chi_{B,j}^D(\theta)}{\sqrt{\lambda_j}}\phi_j^T \Sigma_{H(\mathbf{x})\chi} \\ H_C(\mathbf{x},\theta) \approx \hat{H}_C(\mathbf{x},\theta) = \mu_C + \sigma_C \displaystyle\sum_{j=1}^{N} \frac{\chi_{C,j}^D(\theta)}{\sqrt{\lambda_j}}\phi_j^T \Sigma_{H(\mathbf{x})\chi} \end{cases} \tag{15}$$

where λ_j, ϕ_j are the eigenvalue and eigenvector of each Gaussian auto-correlation matrix (as in the case of non-correlated random fields). Notice that the length of the vector ϕ_j^T and $\mathbf{\Sigma}_{H(\mathbf{x})\chi}$ are equivalent to the number M_{grid} of the grid points (e.g., if the random fields are distributed with all quadrangle shapes, $M_{grid} = M_x * M_y$, with M_x and M_y are the total point numbers in the horizontal (x-axis) and vertical one (y-axis), respectively). In our study, M_{grid} is the total number of all cell centroids.

2.4. Numerical application

The EOLE discretization technique as developed in the previous paragraph, is computed in MATLAB code whilst the analysis process is conducted via open-source Code_Aster. Each time the numerical simulation by Aster code is run, inputs are taken from MATLAB, and the results from Aster are automatically collected and synthesized by MATLAB.

Application to our considered problem, the 2D geometry of deep drift excavated in the COx claystone (Fig. 1), is discretized into 8448 cell elements, and each element is assigned a set of four parameters of COx properties generated from the discretization of four random fields by EOLE. For example, to present the discretized random field of Young's modulus (E), each cell is assigned an arbitrary value of E at its center. This random value is generated by EOLE to perform the aleatoric uncertainty instead of using only the epistemic uncertainty, the subject recently studied in our previous contribution [6]. Note that, in the EOLE process, the values of the truncated order of expansion (N) and the correlation length are two main factors for assessing and controlling the accuracy of the discretization methods. These factors significantly affect the pointwise estimator for variance error of the discretization. Indeed, the EOLE method always under-represents the actual variance of the random field. Thus, the accuracy of this method is strongly correlated with both factors.

It is worth noting also that, for the practical simulation, to reduce the EOLE pointwise error variance at the boundaries, we extend the random field mesh with a small value, e.g., 3.0 m (i.e., the border of the random filed domain $[-3.0, 58]$ m). Besides, each element size must be sufficiently refined (i.e., $L_{RF}/\theta \leq 1/6$ where L_{RF} and θ are the typical element length of random field mesh and the correlation length, respectively [25]).

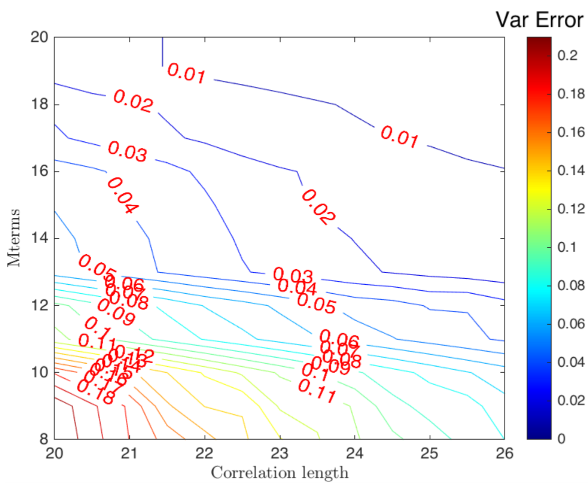

Figure 2. Contour plot of the variance error w.r.t the index of the expansion order (*Mterms* or N) for different values of the correlation length

Fig. 2 shows the relationship between increasing expansion order (N) and the correlation lengths in isotropic cases $\theta_x = \theta_y$ (where θ_x and θ_y are correlation lengths in x- and y-axis, respectively) with variance error max varies from 1% to 20%. Following that, if we set the maximum variance error (i.e., the maximum variance error of all cell positions of the field that we discretized by the EOLE method) to 5%, and then the correlation length is chosen to be 25 m, the truncated order of expansion N (noted as *Mterms* in Fig. 2) must not less than 12 (to ensure the variance less than 0.05). Fig. 3 presents the spatial distribution obtained from a realization of the discretized isotropic variability of the COx rock properties in which an isotropic correlation length of 25 m is adopted. The heterogeneous distribution of these four input parameters presents the consequence of the spatial variability of the COx rock properties.

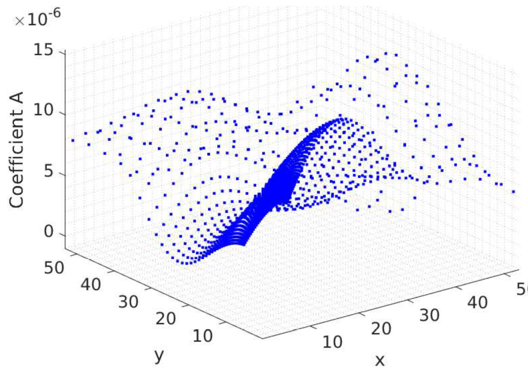

(a) Coefficient A

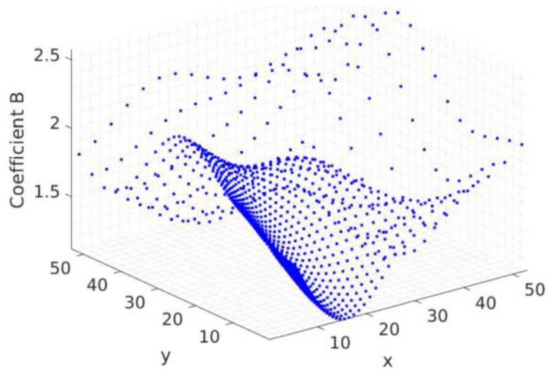

(b) Coefficient B

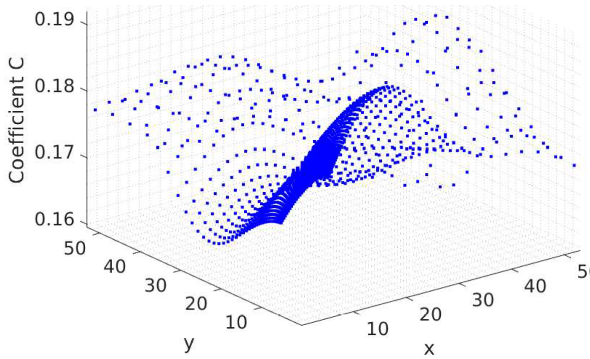

(c) Coefficient C

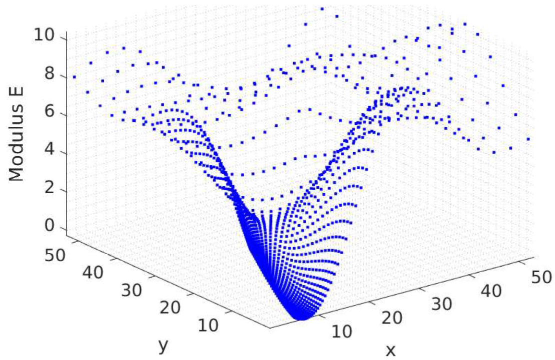

(d) Young's modulus E

Figure 3. Spatial distribution of the mechanical properties of COx rock

3. Stability analysis of deep drift supports

3.1. Results of the deterministic problem

In this section, we present representative results of the deterministic problem using the COx properties provided from one realization of the discretized random fields (i.e., ignoring uncertainty).

As an example, Fig. 4 illustrates the iso values of equivalent stress in the concrete liner of a realization in variability problems by adopting an isotropic correlation length of 25 m. The variability in the space of the viscoplastic properties of the host rock (see Fig. 3) results in, as expected, a heterogeneous distribution of the equivalent stress in this final support of drift. Then, in Fig. 5, we capture the maximum equivalent stress in the concrete liner in time and at 100 years. These results confirm the critical dependence of the stress state in the concrete liner for its chosen thickness. We also highlight in Fig. 6 the effect of the compressibility of the compressible material on the maximum stress in this final support of drift. Like the case of the uncertainty problem (i.e., the issue without considering the variation of the parameter in space) tackled in our recent publication [18], the increase of the compressibility or the thickness of the outer liner allows reducing the maximum equivalent stress in the concrete liner. Nevertheless, it is essential to clarify that the obtained results are only taken from one realization and are not sufficiently representative from a statistical point of view to confirm the observed tendency. The probabilistic results from the following reliability analysis seem much more appropriate for this task.

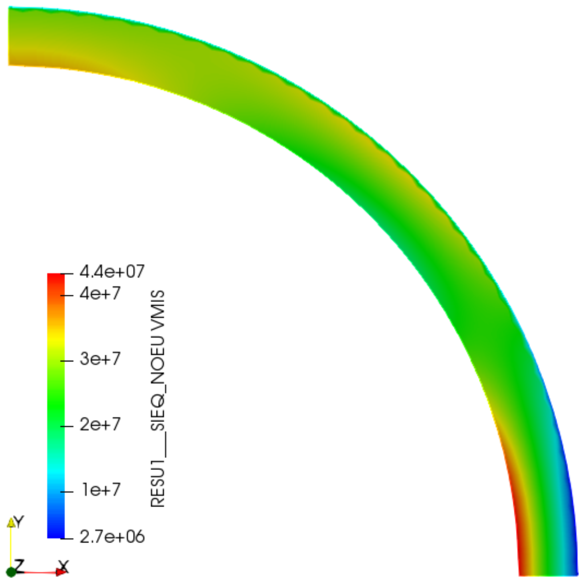

Figure 4. Iso-values of equivalent stress in the concrete liner of a realization in variability problems

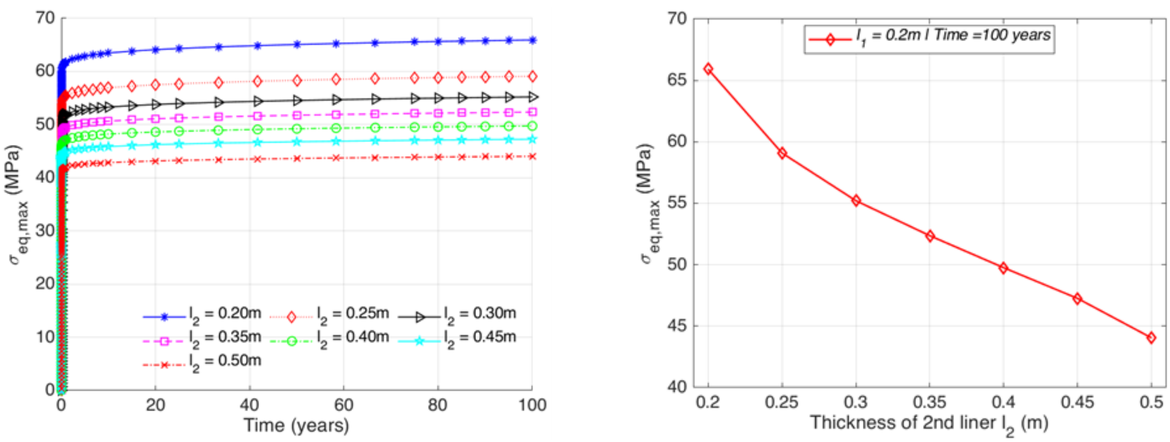

(a) Versus time

(b) At 100 years

Figure 5. Influence of the concrete liner thickness on the maximum equivalent stress for case study 1 with $l_1 = 0.2$ m

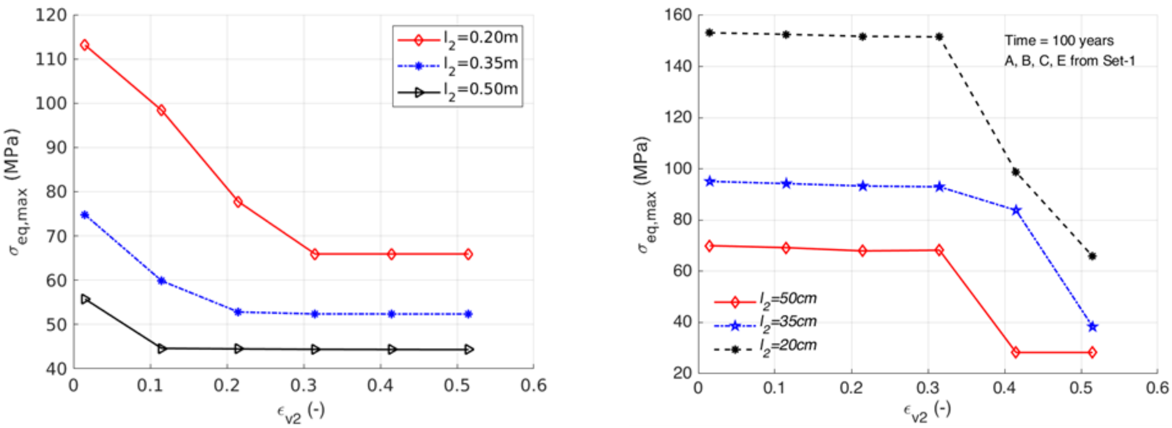

(a) Variability problem

(b) Uncertainty problem taken from the same parameters

Figure 6. Effect of the compressibility of the two-liner thickness on the maximum equivalent stress in the concrete support element ($l_1 = 0.2$ m)

3.2. *Results of the modified AK-MCS reliability analysis*

The modified AK-MCS method, as presented in our previous work [6], is chosen to estimate the stress state's probability of exceedance in the deep drift's concrete liner in the context of spatial variability of COx host rock. From the theoretical point of view, after the discretization of random fields, the problem can be treated similarly to the classical reliability analysis case using different available methods. However, due to the significant increase of the random variables after the discretization, investigating the capability of the chosen reliability analysis method is of primary interest.

Concerning our chosen modified AK-MCS method, it has been shown by some scholars in [37, 38] that it can handle the complex problem with the number of random variables up to about 100. Contrary to these last contributions, which limit only to the academic problems, our study shows that the AK-MCS can only be reasonably applied when the maximum number of variables is about 50. Beyond this number, we state a drastic increase in the training points in the Design of Experiment (DoE) and the time-consuming construction of the Kriging surrogate.

Fig. 7 highlights the results of the reliability analysis when the stress exceedance probability in the concrete liner is predicted as a function of the allowable stress. In current design of Cigeo project, the allowable stress or stress criterion for the concrete liner is $\sigma_{lim2} = 36$ MPa. In these simulations, only the spatial variability of the coefficient A and Young's modulus E (the most affected parameters following our previous study [18]) are considered to limit the total number of random variables at 50 (w.r.t. the truncated order term $N = 25$). More precisely, regarding the formula (Eq. (14) and Eq. (15)), only the random variables $\left\{\xi^A\right\}_{25\times1}$ and $\left\{\xi^E\right\}_{25\times1}$ are activated while zero value is applied for all the elements of the other random variables $\left\{\xi^B\right\}_{25\times1}$ and $\left\{\xi^C\right\}_{25\times1}$ (i.e., the two parameters B and C have kept constants at their mean values).

Table 1 is summarized the exceedance probability at 100 years in the concrete liner (with the thickness of 50 cm) between uncertainty and variability problems (i.e., a case considering the spatial variability COx rock properties). It illustrates that in the variability problem (with the isotropic correlation length of 50 m), the exceedance probability value ($P_f = 0.098\%$) is slightly smaller than the

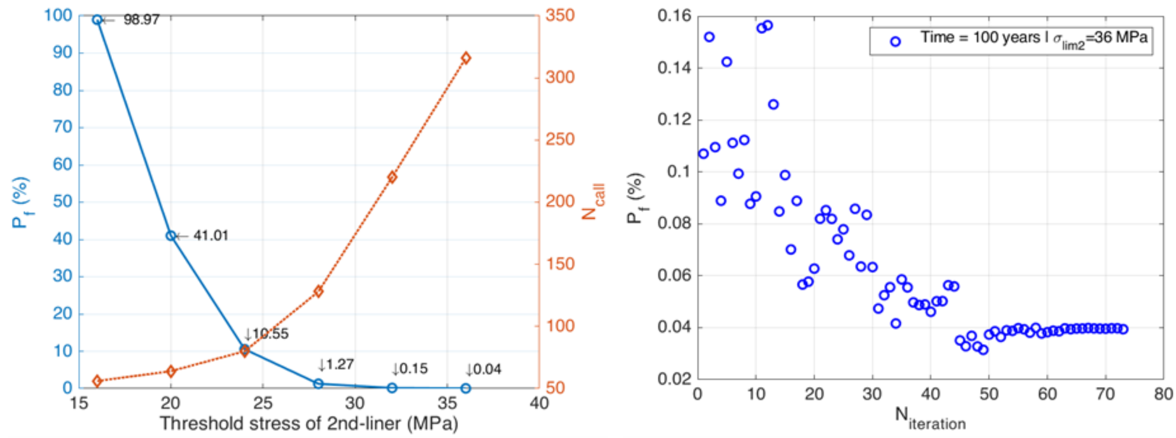

(a) Versus threshold stresses of 2 nd liner

(b) Versus iteration numbers for allowable stress σ_{lim2} = 36 MPa

Figure 7. Stress exceedance probability at 100 years in the concrete liner

relevant case of uncertainty problem (P_f = 0.11%) evaluated in our previous research [18]. This point highlights the spatial variability effect of the COx rock properties on the exceedance probability of the concrete liner of drift. However, this observation must be strengthened in the intensively numerical investigations taking into account different values of correlation length of COx rock properties (e.g., smaller correlation length) and of the concrete liner thickness as well as with a more appropriate geometrical model of drift (e.g., the total 2D plane strain model without symmetric conditions or in the general 3D problems). For this purpose, more extensions of the reliability analysis methodology must be conducted to treat the problem of the very high dimensional problem.

Table 1. Comparison of exceedance probability of concrete liner between uncertainty and variability problems

Study case	Number of variables ($4 * N$)	N_{call}	P_f (%)
Uncertainty (as in [18])	$4 * 1$	296	0.13
Variability (Isotropic correlation length 50 m)	$4 * 6$	488	0.098

4. Conclusions

The long-term stability of an underground structure like the deep drift excavated in the COx claystone is considered in the context of a deep geological disposal facility by accounting for spatial variability of the viscoplastic properties of the host rock. The creep behavior of the rock mass is described by Lemaitre law and characterized by three parameters. The random field concept is adopted to present the variability in the space of each mechanical parameter of the host rock. An extension of the well-known EOLE method is undertaken to discretize the cross-correlated random fields. The reliability analysis is then conducted on the discretized random fields. The modified AK-MCS method is chosen for this reliability analysis. It seems only appropriate for tackling the variability problem owing to a high correlation length characterized by a low or moderate number (up to about 50) of random variables after the discretization. Compared to the uncertainty problem, the spatial variability gives a lower stress exceedance probability of stress state in the drift support. However, this statement must be investigated in the other cases with smaller correlation lengths and in the general 3D simulations. Further future works can be consisted of dealing with the high dimensional problem resulting from the considered spatial-temporal variability. The developments/extensions of the metamodeling technique with respect to time variables present an interesting tool to consider more complex problems, which incorporate, for instance, the thermo-hydro-mechanical coupling as well as the degradation mechanism of liners.

References

[1] Fenton, G. A., Griffiths, D. V. (2008). *Risk assessment in geotechnical engineering*. John Wiley & Sons, Inc.

[2] Al-Bittar, T., Soubra, A.-H. (2012). Bearing capacity of strip footings on spatially random soils using sparse polynomial chaos expansion. *International Journal for Numerical and Analytical Methods in Geomechanics*, 37(13):2039–2060.

[3] Xiao, T., Li, D.-Q., Cao, Z.-J., Tang, X.-S. (2016). Full probabilistic design of slopes in spatially variable soils using simplified reliability analysis method. *Georisk: Assessment and Management of Risk for Engineered Systems and Geohazards*, 11(1):146–159.

[4] Li, D.-Q., Xiao, T., Cao, Z.-J., Phoon, K.-K., Zhou, C.-B. (2016). Efficient and consistent reliability analysis of soil slope stability using both limit equilibrium analysis and finite element analysis. *Applied Mathematical Modelling*, 40(9-10):5216–5229.

[5] Song, K.-I., Cho, G.-C., Lee, S.-W. (2011). Effects of spatially variable weathered rock properties on tunnel behavior. *Probabilistic Engineering Mechanics*, 26(3):413–426.

[6] Tran, N.-T., Do, D.-P., Hoxha, D., Vu, M.-N., Armand, G. (2022). Modified AK-MCS method and its application on the reliability analysis of underground structures in the rock mass. *Journal of Science and Technology in Civil Engineering (STCE) - HUCE*, 16(2):38–54.

[7] Griffiths, D. V., Fenton, G. A. (2004). Probabilistic slope stability analysis by finite elements. *Journal of Geotechnical and Geoenvironmental Engineering*, 130(5):507–518.

[8] Yu, X., Cheng, J., Cao, C., Li, E., Feng, J. (2019). Probabilistic analysis of tunnel liner performance using random field theory. *Advances in Civil Engineering*, 2019:1–18.

[9] Kim, H.-S., Major, G., Ross-Brown, D. (1978). Application of Monte Carlo techniques to slope stability analyses. In *19th US Symposium on Rock Mechanics (USRMS)*, OnePetro.

[10] Fenton, G. A. (1999). Estimation for stochastic soil models. *Journal of Geotechnical and Geoenvironmental Engineering*, 125(6):470–485.

[11] Haldar, S., Babu, G. L. S. (2008). Effect of soil spatial variability on the response of laterally loaded pile in undrained clay. *Computers and Geotechnics*, 35(4):537–547.

[12] Lü, Q., Xiao, Z., Zheng, J., Shang, Y. (2018). Probabilistic assessment of tunnel convergence considering spatial variability in rock mass properties using interpolated autocorrelation and response surface method. *Geoscience Frontiers*, 9(6):1619–1629.

[13] Song, K.-I., Cho, G.-C., Lee, S.-W. (2011). Effects of spatially variable weathered rock properties on tunnel behavior. *Probabilistic Engineering Mechanics*, 26(3):413–426.

[14] Tran, N.-T., Do, D.-P., Hoxha, D., Vu, M.-N. (2019). Reliability-based design of deep tunnel excavated in the viscoelastic Burgers rocks. In *Lecture Notes in Civil Engineering*, Springer Singapore, 375–382.

[15] Tran, N. T. (2020). Long-term stability evaluation of underground constructions by considering uncertainties and variability of rock masses. PhD thesis, Orleans University, France.

[16] Sudret, B. (2007). Uncertainty propagation and sensitivity analysis in mechanical models–Contributions to structural reliability and stochastic spectral methods. *Habilitationa diriger des recherches, Université Blaise Pascal, Clermont-Ferrand, France*, 147:53.

[17] Do, D. P., Tran, N. T., Hoxha, D., Vu, M. N., Armand, G. (2021). Kriging-based optimization design of deep tunnel in the rheological Burger rock. *IOP Conference Series: Earth and Environmental Science*, 833(1):012155.

[18] Tran, N.-T., Do, D.-P., Hoxha, D., Vu, M.-N., Armand, G. (2021). Kriging-based reliability analysis of the long-term stability of a deep drift constructed in the Callovo-Oxfordian claystone. *Journal of Rock Mechanics and Geotechnical Engineering*.

[19] Do, D.-P., Vu, M.-N., Tran, N.-T., Armand, G. (2021). Closed-form solution and reliability analysis of deep tunnel supported by a concrete liner and a covered compressible layer within the viscoelastic burger rock. *Rock Mechanics and Rock Engineering*, 54(5):2311–2334.

[20] Tran, N. H., Do, D. P., Vu, M. N., Nguyen, T. T. N., Pham, D. T., Trieu, H. T. (2022). Combined effect of anisotropy and uncertainty on the safe mud pressure window of horizontal wellbore drilled in anisotropic saturated rock. *International Journal of Rock Mechanics and Mining Sciences*, 152:105061.

[21] Mánica, M. A., Gens, A., Vaunat, J., Armand, G., Vu, M.-N. (2021). Numerical simulation of underground excavations in an indurated clay using non-local regularisation. Part 1: formulation and base case. *Géotechnique*, 1–21.

[22] Yu, Z., Shao, J., Duveau, G., Vu, M.-N., Armand, G. (2021). Numerical modeling of deformation and damage around underground excavation by phase-field method with hydromechanical coupling. *Computers and Geotechnics*, 138:104369.

[23] Li, C.-C., Kiureghian, A. D. (1993). Optimal discretization of random fields. *Journal of Engineering Mechanics*, 119(6):1136–1154.

[24] Allaix, D. L., Carbone, V. I. (2009). Discretization of 2D random fields: A genetic algorithm approach. *Engineering Structures*, 31(5):1111–1119.

[25] Sudret, B., Der Kiureghian, A. (2000). *Stochastic finite element methods and reliability: a state-of-the-art report*. University of Calif Ornia Berkeley, 189.

[26] Kiureghian, A. D., Ke, J.-B. (1988). The stochastic finite element method in structural reliability. *Probabilistic Engineering Mechanics*, 3(2):83–91.

[27] Fenton, G. A., Vanmarcke, E. H. (1990). Simulation of random fields via local average subdivision. *Journal of Engineering Mechanics*, 116(8):1733–1749.

[28] Phoon, K. K., Huang, S. P., Quek, S. T. (2002). Implementation of Karhunen–Loeve expansion for simulation using a wavelet-Galerkin scheme. *Probabilistic Engineering Mechanics*, 17(3):293–303.

[29] Sudret, B., Kiureghian, A. D. (2002). Comparison of finite element reliability methods. *Probabilistic Engineering Mechanics*, 17(4):337–348.

[30] Cho, S. E. (2010). Probabilistic assessment of slope stability that considers the spatial variability of soil properties. *Journal of Geotechnical and Geoenvironmental Engineering*, 136(7):975–984.

[31] Jiang, S.-H., Li, D.-Q., Zhang, L.-M., Zhou, C.-B. (2014). Slope reliability analysis considering spatially variable shear strength parameters using a non-intrusive stochastic finite element method. *Engineering Geology*, 168:120–128.

[32] Huang, H. W., Xiao, L., Zhang, D. M., Zhang, J. (2017). Influence of spatial variability of soil Young's modulus on tunnel convergence in soft soils. *Engineering Geology*, 228:357–370.

[33] Allaix, D. L., Carbone, V. I. (2010). Numerical discretization of stationary random processes. *Probabilistic Engineering Mechanics*, 25(3):332–347.

[34] Haj, A.-K. E., Soubra, A.-H., Fajoui, J. (2019). Probabilistic analysis of an offshore monopile foundation taking into account the soil spatial variability. *Computers and Geotechnics*, 106:205–216.

[35] Zhao, T., Wang, Y. (2018). Simulation of cross-correlated random field samples from sparse measurements using Bayesian compressive sensing. *Mechanical Systems and Signal Processing*, 112:384–400.

[36] Vořechovský, M. (2008). Simulation of simply cross correlated random fields by series expansion methods. *Structural Safety*, 30(4):337–363.

[37] Lelièvre, N. (2018). *Development of AK-based method for reliability analyses*. Université Clermont Auvergne.

[38] Wang, Q., Fang, H. (2020). An adaptive high-dimensional model representation method for reliability analysis of geotechnical engineering problems. *International Journal for Numerical and Analytical Methods in Geomechanics*, 44(12):1705–1723.